*Am J Physiol Renal Physiol* 295: F380–F387, 2008.
First published May 7, 2008; doi:10.1152/ajprenal.00598.2007.

# MiRP3 acts as an accessory subunit with the BK potassium channel

**Daniel I. Levy,[1] Sherry Wanderling,[1] Daniel Biemesderfer,[2] and Steve A. N. Goldstein[3,4]**

*Departments of [1]Medicine and [3]Pediatrics, and [4]Institute for Molecular Pediatric Sciences, Biological Sciences Division, University of Chicago, Chicago, Illinois; and [2]Department of Internal Medicine, School of Medicine, Yale University, New Haven, Connecticut*

Submitted 18 December 2007; accepted in final form 2 May 2008

**Levy DI, Wanderling S, Biemesderfer D, Goldstein SA.** MiRP3 acts as an accessory subunit with the BK potassium channel. *Am J Physiol Renal Physiol* 295: F380–F387, 2008. First published May 7, 2008; doi:10.1152/ajprenal.00598.2007.—MinK-related peptides (MiRPs) are single-span membrane proteins that assemble with specific voltage-gated $K^+$ (Kv) channel α-subunits to establish gating kinetics, unitary conductance, expression level, and pharmacology of the mixed complex. MiRP3 (encoded by the *KCNE4* gene) has been shown to alter the behavior of some Kv α-subunits in vitro but its natural partners and physiologic functions are unknown. Seeking in vivo partners for MiRP3, immunohistochemistry was used to localize its expression to a unique subcellular site, the apical membrane of renal intercalated cells, where one potassium channel type has been recorded, the calcium- and voltage-gated channel BK. Overlapping staining of these two proteins was found in rabbit intercalated cells, and MiRP3 and BK subunits expressed in tissue culture cells were found to form detergent-stable complexes. Electrophysiologic and biochemical evaluation showed MiRP3 to act on BK to reduce current density in two fashions: shifting the current-voltage relationship to more depolarized voltages in a calcium-dependent fashion (~10 mV at normal intracellular calcium levels) and accelerating degradation of MiRP3-BK complexes. The findings suggest a role for MiRP3 modulation of BK-dependent urinary potassium excretion.

*KCNE4*; *KCNMA1*; MaxiK; slo; intercalated cells

MINK AND THE MINK-RELATED peptides (MiRPs) are proteins with a single transmembrane span that associate with potassium channels to modulate their function (3, 4). The importance of these proteins to normal physiology of the heart and nervous system is exposed by their association with clinical disorders such as congenital long QT syndrome, drug-induced cardiac arrhythmias, sensorineural deafness, and periodic paralysis (1, 4, 48, 49, 51). In addition, MiRPs influence the normal physiology of endocrine and exocrine glands, intestinal secretion, and renal excretion (32). Because the peptides are promiscuous in their roles and interact with a wide variety of potassium channels (2), careful evaluation is required to delineate bona fide (in vivo) relationships. Thus, the capacity of a specific MiRP to alter function of a channel complex in vitro does not necessarily correlate with their interaction in vivo (33).

MinK-related peptide 3 (MiRP3), encoded by the *KCNE4* gene, enjoys broad mRNA expression in mice and humans (20, 31) and a role in human heart has been suggested (7, 19, 29, 46). Here, we undertook an approach to identifying physiological partners for MiRP3 similar to that used previously for MiRP1 and MiRP2 (1, 4). Polyclonal antibodies were raised and used to localize MiRP3 to a particular cell type and locale in vivo. Thereafter, potassium channels known to operate at the site were evaluated. Thus, MiRP3 was localized to the specialized apical membrane of renal intercalated (IC) cells where the only potassium channel characterized to date is the voltage- and calcium-gated BK channel (39, 40, 62). Functional partnership of MiRP3 and BK was therefore evaluated. Studies in cultured cells revealed mono-glycosylation and type I membrane orientation of MiRP3, stable complex formation of MiRP3 and BK, and MiRP3 reduction of BK currents due to a shift in the current-voltage relationship to more depolarized voltages, ~10 mV at 0.1 μM intracellular calcium ($[Ca^{2+}]_i$), and enhanced channel degradation. The effect of MiRP3 on activation is similar to that seen with *KCNMB*-encoded BK accessory subunits (proteins with 2 transmembrane spans), and the control of channel half-life may be similar to a form of channel regulation by KCNMB1 that was recently described (54). A role for MiRP3 in urinary potassium excretion is considered.

## EXPERIMENTAL PROCEDURES

*Molecular biology.* The coding regions of human, rat, and rabbit *KCNE4* genes (NCBI NM_080671, AF512994, and AY926882, respectively) were cloned from cDNA libraries and subcloned with a Kozak consensus sequence (GCCACC) before initiating the methionine codon into a vector (pRAT) that is optimized for both oocyte and mammalian expression (10). Plasmids containing human *KCNMA1* and *KCNMB1* (NCBI U11058 and NM_004137, respectively) were gifts from Dr. L. Toro and these genes were cloned into pRAT as described for *KCNE4*. An epitope-tagged variant of BK was engineered by introducing a linker (RVPDGDPD) followed by the bacterial rhodopsin sequence, 1d4 (ETSQVAPA), at the COOH terminus.

*Antibody development.* Three epitopes of the MiRP3 cytoplasmic tail were chosen for generation of polyclonal antibodies, consisting of amino acid residues 67-138, 136-150, and 151-170. These epitopes are largely conserved across human, rat, and rabbit homologs. A GST fusion protein was produced that contained residues 67-138, after subcloning the encoding nucleotide sequence in frame into the multiple cloning site of pGEX 6p-1. The two other epitopes were generated by conjugating synthetic peptides to keyhole limpet hemocyanin (Calbiochem, San Diego, CA) (21). The immunogens were used for inoculation of rabbits by Pocono Rabbit Farms & Laboratories (Canadensis, PA). The serum immunoglobulins were purified with protein A sepharose beads (Amersham Biosciences, Piscataway, NJ), and affinity purification of the anti-MiRP3 antibodies was made with immobilized antigens.

Address for reprint requests and other correspondence: S. A. N. Goldstein or D. I. Levy, Univ. of Chicago, Section of Nephrology, MC5100, 5841 S. Maryland Ave., Chicago, IL 60637-1447 (e-mail: sangoldstein@uchicago.edu or dlevy@medicine.bsd.uchicago.edu).

The costs of publication of this article were defrayed in part by the payment of page charges. The article must therefore be hereby marked "*advertisement*" in accordance with 18 U.S.C. Section 1734 solely to indicate this fact.

  

*Immunohistochemistry.* All animal experimentation was conducted in accordance with the *Guide for the Care and Use of Laboratory Animals* (National Institutes of Health, Bethesda, MD) and was approved by the local Institutional Animal Care and Use Committees. Rats were fed normal or high potassium diets (1 and 5% wt/wt, respectively) and rabbits were fed a high potassium (5% wt/wt) diet for 7–10 days before death. Their kidneys were fixed in 2.5% paraformaldehyde, cryopreserved with 15% sucrose, and embedded in Cryo-Gel (Instrumedics, St. Louis, MO) before being sectioned at 5 μm. Epitope retrieval was performed with 10 mM sodium citrate, pH 6.0, and sections were subsequently permeabilized with 0.25% Triton X-100 and 0.1% Tween-20 in phosphate-buffered saline and blocked with 10% donkey serum. Rat sections were incubated for 1 h at room temperature with mouse anti-anion exchanger 1 (AE1) at 1:100 (IVF12; University of Iowa Developmental Hybridoma Bank) and either rabbit anti-MiRP3$_{136\text{-}150}$ at 1:500 or rabbit anti-MiRP3$_{151\text{-}170}$ at 1:250. This was followed by Alexa Fluor 488 donkey anti-mouse 1:600 and Alexa Fluor 594 donkey anti-rabbit 1:600 (Invitrogen, Carlsbad, CA) secondary antibodies. Rabbit sections were incubated with primary antibodies overnight at 4°C: chicken anti-BK (37) at 1:200 (a gift from Dr. T. Kleyman), rabbit anti-aquaporin-2 (63) at 1:30,000 (a gift from M. Cadnapaphornchai), and goat anti-MiRP3 at 1:100 (KCNE4 N-14; Santa Cruz Biotechnology, Santa Cruz, CA) followed by respective secondary antibodies for 1 h at room temperature: Texas Red donkey anti-chicken 1:300 (Jackson Immunoresearch, West Grove, PA), Alexa Fluor 488 donkey anti-rabbit 1:600, and Alexa Fluor 647 donkey anti-goat 1:300 (Invitrogen). All samples were mounted with Vectashield hard set mounting medium (Vector Laboratories, Burlingame, CA) and imaged with a ×63 objective.

*Biochemistry.* Rat hearts and kidneys were obtained frozen from Pel-Freez (Rogers, AR). Tissue was homogenized in lysis buffer (in mM): 100 NaCl, 40 KCl, 20 K-HEPES, 1 Na-EDTA, 10% vol/vol glycerol, and protease inhibitor tablets (Roche Applied Science, Indianapolis, IN), pH 7.4, and then solubilized by adding 2% Triton X-100 (Roche Applied Science). After centrifugation to remove insoluble materials, lysates were fractionated by SDS-PAGE.

Transformed African green monkey kidney fibroblast cells (COS-7) and Chinese hamster ovary K-1 (CHO) cells were cultured in DMEM and α-MEM (Invitrogen), respectively, supplemented with 10% FBS and held at 37°C in humidified air with 5% $CO_2$. Cells were transfected for biochemistry with 10–20 μg of plasmid DNA in 150-mm dishes by adding 2 μl Lipofectamine 2000 (Invitrogen) per 1 μg DNA in 3 ml of Opti-MEM added to 15 ml of medium. The cells were rinsed with fresh culture medium after 2 h and harvested 12–36 h later. Pellets of harvested cells were solubilized for 1 h in lysis buffer containing 1% Triton X-100, and insoluble material was removed by centrifugation. Immunopurification of epitope-tagged BK was performed as before by Kim et al. (25) with anti-1d4 monoclonal antibody (National Cell Culture Center, Minneapolis, MN) linked to sepharose beads and elution with 1 mg/ml 1d4 peptide.

Steady-state biotinylation experiments used CHO cells transfected with vector for wild-type BK channels along with an equal concentration of vector that was empty or carried *KCNE4*. Twenty-four hours after transfection, cells were incubated with 1.5 mM sulfo-NHS-SS-biotin (Pierce, Rockford, IL) in PBS (pH 8.0) for 30 min at room temperature. Cells were rinsed and solubilized and samples were diluted to normalize total protein concentration. Biotin-labeled proteins were isolated by incubation with streptavidin beads (Pierce) for 1 h at 4°C and liberated by incubation with 4× SDS-PAGE sample buffer with 200 mM dithiothreitol for 15 min at 55°C.

Pulse-chase experiments were carried out by transfecting CHO cells with vector for the 1d4-tagged variant of BK along with an equal concentration of second vector that was empty or carried *KCNE4* or the similarly sized Iip35 coding sequence. Because the length of the empty vector is ~10% shorter than the *KCNE4* or Iip35 vectors, there was a 10% greater number of copies of the second vector in the control group. Twelve hours after transfection, cells were starved for 1 h in pulse media: thiol-free DMEM (Invitrogen) supplemented with 1 mM pyruvate, 2 mM glutamine, and 10% dialyzed FBS; this was followed by a 1-h incubation in pulse media containing 150 μCi/ml of $^{35}$S-labeled methionine and cysteine (Pro-mix, Amersham Biosciences). After the pulse, cells were rinsed with α-MEM supplemented with 2 mM cold methionine and cysteine. The cells for the 1-h time point were biotinylated as above and the remaining dishes of cells were chased under normal culture conditions until biotinylation. After biotinylation, cells were harvested, pelleted, and frozen at −80°C until all groups of cells were simultaneously lysed for BK-1d4 purification with sepharose beads covalently linked to 1d4 antibody. A small sample of lysates was saved for estimation of total incorporated radioactive label by trichloroacetic acid (TCA) precipitation and used to assess $^{35}$S incorporation and cell recovery. After 1d4 peptide elution, 15% of the purified BK was saved for electrophoresis and the remainder was used for purification of the surface component. The samples were analyzed by SDS-PAGE and autoradiography (Storm 860, Amersham Biosciences), and values for radiolabeled BK were scaled to TCA precipitable counts using an interpolated line of decay to control for recovery of sample. Half-life was determined by fitting BK expression from 6 to 16 h with the function $y = y_o \cdot 2^{-x/T}$, where $T$ is the half-life of BK counts (h) and $y_o$ represents the $y$-intercept.

*Western blotting.* Western blots were probed with anti-MiRP3$_{136\text{-}150}$ and a mouse monoclonal antibody to the BK$_{690\text{-}891}$ epitope (35) purchased from the UC Davis/NINDS/NIMH NeuroMab Facility (Davis, CA). Blots were imaged on a Licor Odyssey (Lincoln, NE) using fluorescent secondary antibodies, and bands were quantified via Odyssey software.

*Patch-clamp experiments.* CHO cells were prepared for electrophysiology by transfecting and then plating onto glass coverslips in 35-mm culture dishes. The transfections were performed with an additional vector encoding a variant of green fluorescent protein, pEGFP (Clontech, Palo Alto, CA). Transfected cells were identified as those with green fluorescence during brief illumination with a mercury lamp, and typically represented 20% of the total population of cells. All recordings were made in the inside-out mode using an Axopatch 200A amplifier (Axon Instruments) and CLAMPEX software. Macroscopic recordings of 0.4–6.0 nA were made with borosilicate electrodes of 1- to 4-MΩ resistance, and single-channel recordings were made with ~8-MΩ electrodes. Data acquisition began ~10 min after pulling off the patch, once it was established that the conductance-voltage ($G$-$V$) relationship was stable in the experimental solution.

Pipette solution contained (in mM) 105 KOH, 10 HEPES, 5 KCl, 2 *N*-(2-hydroxyethyl)ethylenediamine-*N*,*N*′,*N*′-triacetic acid (HEDTA), 10 μM free $Ca^{2+}$, pH 7.20, with methanesulfonic acid. The bath solution was identical except that $CaCl_2$ was added to achieve a range of free $Ca^{2+}$ between 0.1 and 50 μM, as calculated by MaxChelator software (41), and titrated with a calcium electrode (Thermo-Orion, Beverly, MA). All solutions were held in plastic containers to prevent leeching of calcium from glass bottles.

## RESULTS

*MiRP3 is expressed on the apical membrane of renal IC cells and colocalizes with the BK channel.* Rabbit polyclonal antibodies were generated against three distinct amino acid sequences in the cytoplasmic tail of MiRP3 that share at least 90% identity in human, mouse, and rat isoforms. Antibodies were affinity-purified on peptide antigen and proved useful for Western blotting and immunohistochemistry. Based on reports of *KCNE4* mRNA expression in kidney (19, 20, 53), ultrathin sections of rat kidney were stained (8, 9), localizing MiRP3 protein to the apical (luminal) membranes of IC cells of renal cortex and medulla (Fig. 1*A*). The stained cells were identified as type A IC cells by their morphology, number, and counter-

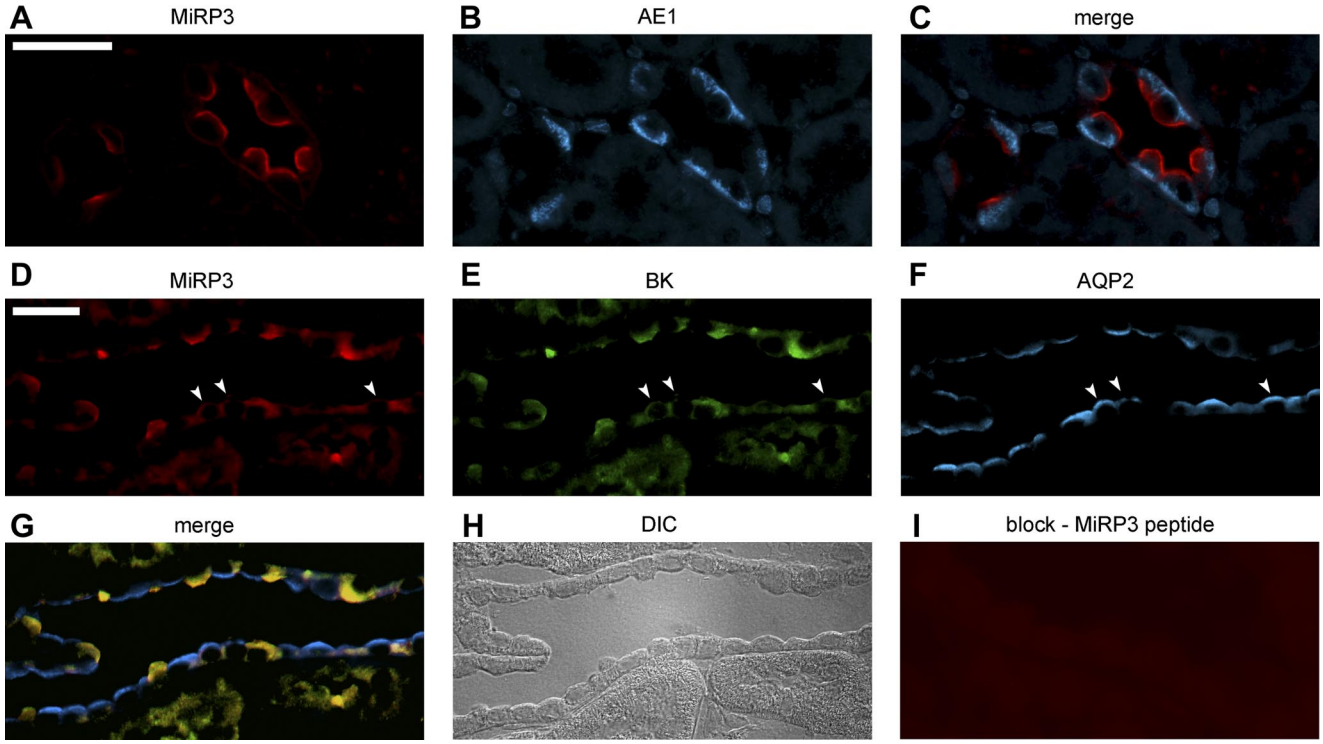


Fig. 1. MiRP3 expression in the kidney colocalizes with BK channel to the apical membrane of intercalated (IC) cells. Staining of rat kidney cortex (*top*) shows localized expression of MiRP3 (anti-MiRP3$_{136\text{-}150}$; *A*) on the apical membrane of IC cells and expression of the chloride-bicarbonate exchanger AE1 (*B*) on the basolateral membrane of the same cells (merge; *C*). This staining pattern was also found with the anti-MiRP3$_{151\text{-}170}$ antibody (not shown). Coexpression of MiRP3 and BK channel is shown in rabbit renal cortex (*middle* and *bottom*) with goat anti-MiRP3 (*D*), chicken anti-BK (*E*), rabbit anti-aquaporin 2 (*F*; merged image, *G*), using the anti-aquaporin antibody as a marker for the adjacent principal cells. A DIC image (*H*) of the tubule shown in *D–G* is presented to aid in cell identification. Peptide against MiRP3 (*I*) was used to show specificity of the antibody. Scale bars indicate a distance of 25 μm, and arrowheads point to principal cells that stain weakly for MiRP3 and BK.

staining of the basolateral membrane with a monoclonal antibody to the chloride-bicarbonate exchanger, AE1 (Fig. 1, *B* and *C*) (5, 52). Because virtually all cells staining for AE1 also stained for MiRP3, it is likely that MiRP3 is present in both connecting tubule (CNT) and collecting ducts (24). Staining was judged to be specific, as a similar signal was found for antibodies to two MiRP3 epitopes and signal was eliminated when MiRP3 antibodies were preincubated with antigen (not shown). Focal expression of MiRP3 on IC apical membranes suggested it might interact with BK potassium channels which had previously been localized to this specialized membrane by electrophysiology (39, 40) and immunohistochemistry (62). Colocalization of MiRP3 and BK channels was attempted in rat kidney, but anti-BK antibodies were not effective for staining rat kidney, even when tissue was taken from rats on a high potassium diet.

MiRP3 and BK were subsequently colocalized in IC cells of rabbit kidney. Using goat anti-MiRP3, chicken anti-BK, and rabbit anti-AQP2 antibodies, strong MiRP3 expression on the apical surface of IC cells was confirmed in rabbit cortex and medulla and found to costain with BK (Fig. 1, *D–H*). In rabbit kidney, however, there was also weak staining of BK and MiRP3 in some principal cells (arrowheads, Fig. 1, *D* and *E*). This expression pattern has been noted for BK in rabbit kidney (37, 62). Staining was lost when either MiRP3 or BK antibodies were preincubated with blocking peptide (Fig. 1*I*, for MiRP3 antibodies). MiRP3 antibody also identified IC cells when no BK antibody was used and BK was similarly identified when no MiRP3 antibody was used (not shown). Although BK is known to be expressed in vascular smooth muscle, we did not detect BK staining of renal vessels.

*MiRP3 is a glycosylated type I protein.* MiRP3 protein in rat tissue lysates and heterologously expressed in CHO cells was evaluated by Western blot analysis. Two specific bands were visualized at 22–28 kDa from heart, kidney, and cells transfected with human MiRP3 but not with vector-transfected cells, using antibodies to MiRP3$_{136\text{-}150}$ or MiRP3$_{151\text{-}170}$ epitopes (Fig. 2*A*), consistent with findings of Manderfield and George (31); bands were specifically eliminated by preincubation of antibodies with immunizing antigen (not shown). Native MiRP3 showed a larger apparent mass than heterologously expressed protein suggesting differences in posttranslational modification.

Treatment of heterologously expressed MiRP3 with the deglycosidase PNGase F led to an ~2-kDa decrease in the apparent mass, as did mutation of the asparagine at MiRP3 position 8 to glutamine (MiRP3 N8Q) removing the single canonical consensus sequence for N-linked glycosylation (Fig. 2*B*). Migration of MiRP3 N8Q was not modified by PNGase F treatment. These findings suggest that native MiRP3 is glycosylated in native tissues and is a type I membrane protein (that is, bearing an external $NH_2$ terminus) like other members of KCNE family (1, 4, 13).

*MiRP3 and BK stably interact within cells.* Because MiRP3 and BK are expressed on the same cell membrane, MiRP3 was overexpressed in CHO cells with a variant of human BK modified to carry the 1d4 epitope on its COOH terminus

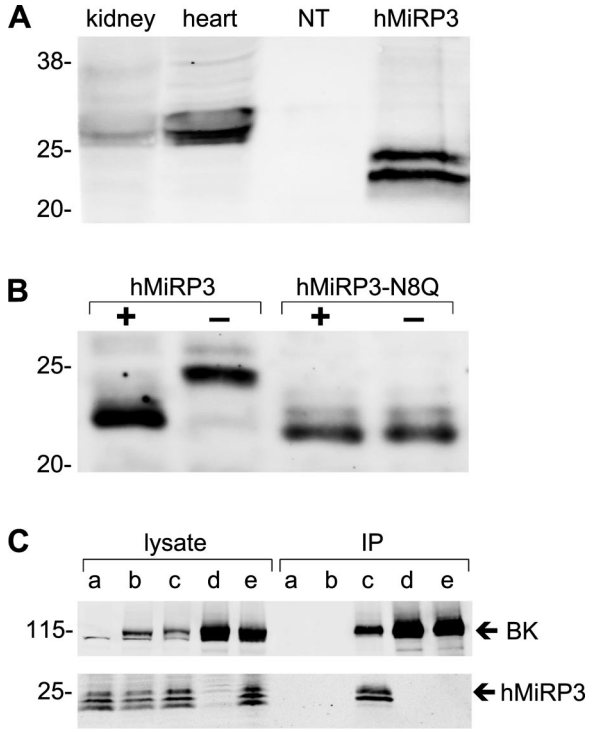


Fig. 2. MiRP3 expression and its copurification with BK. *A*: bands of 22–28 kDa are seen for homogenates of rat heart, rat kidney, and Chinese hamster ovary (CHO) cells transfected with human MiRP3 (hMiRP3). Lysates from CHO cells transfected with empty vector (NT) did not stain for MiRP3. *B*: lysates of COS-7 cells expressing wild-type hMiRP3, incubated for 45 min with PNGase, show a size decrease of ~2 kDa. The migration of hMiRP3-N8Q is equivalent to that of PNGase-treated wild-type protein and unchanged by PNGase treatment. *C*: CHO cells with hMiRP3 (*a*), hMiRP3 and BK (*b*), hMiRP3 and BK-1d4 (*c*), or BK-1d4 alone (*d*) were subjected to lysis and immunopurification with anti-1d4 antibodies. An additional treatment group (*e*) consisted of lysate from cells expressing MiRP3 mixed with lysate from cells expressing BK-1d4, incubated together at 4°C for 16 h before immunopurification (IP). MiRP3 is purified only when coexpressed with BK-1d4.

(BK-1d4). Proteins were purified after detergent lysis of the cells via monoclonal antibodies specific to the tag. Figure 2*C* shows that MiRP3 and BK-1d4 are purified together, indicating that they form detergent-stable complexes when coexpressed. Recovery was specific since MiRP3 was not recovered when the channel had no tag or when MiRP3 or BK-1d4 was expressed alone. Coassembly of BK and MiRP3 within the cells rather than secondarily after solubilization was demonstrated by the inability to copurify MiRP3 after mixing lysates of cells expressing BK-1d4 with cells expressing MiRP3. While total cell lysates reveal a third, smaller MiRP3 band, it appears to be a degradation product because only the expected MiRP3 doublet is isolated via BK-1d4.

*MiRP3 reduces macroscopic but not single-channel BK currents.* Net BK current was greatly reduced when MiRP3 was coexpressed. Representative traces for a family of depolarizing steps from −80 to +80 mV are shown in Fig. 3*A*, and the mean conductance per membrane patch is presented in Fig. 3*B*. With bath $[Ca^{2+}]_i$ of 10 μM, the mean (±SE) conductance at +80 mV was 44.7 ± 16.6 vs. 4.6 ± 2.2 nS for patches from cells transfected with BK without and with MiRP3, respectively ($n = 9$ for each group). Patches were equivalent in size (electrode resistance 3.0 ± 0.2 MΩ for both groups) and were taken from cells bearing similar, moderate fluorescence. As expected, expression of MiRP3 alone yielded no currents since the accessory subunit does not form a channel on its own (Fig. 3*A*).

Possible explanations for reduced BK current include a smaller unitary conductance, a change in the voltage required to activate the channels, and/or decreased expression of BK at the plasma membrane. To assess the mechanism for current reduction, single-channel recordings were performed. Figure 3*C* shows representative recordings of BK (*left*) and BK expressed with MiRP3 (*right*) over a range of membrane potentials with 1 μM $[Ca^{2+}]_i$. Comparing slope conductances of 5 patches in each group (Fig. 3*D*) revealed no change in BK unitary current with MiRP3 (means ± SE conductances were 280 ± 8 and 289 ± 5 pS, for BK without and with MiRP3, respectively).

*MiRP3 shifts BK activation to depolarized potentials in a calcium-dependent manner.* To determine the voltage required to activate BK channels half-maximally ($V_{½\text{-act}}$), various voltages and calcium concentrations were studied. At 10 μM $[Ca^{2+}]_i$, MiRP3 coexpression causes a +22-mV shift of $V_{½\text{-act}}$, from −17.8 ± 7.7 to +4.0 ± 3.9 mV (Fig. 3*E*). In 0.1 μM $[Ca^{2+}]_i$, approximating steady-state intracellular concentration in IC cells (61), the shift in $V_{½\text{-act}}$ was +9 mV, from +62.2 ± 4.1 to +71.1 ± 3.0 mV (means ± SE, $n = 6$ patches each). Half-maximal activation voltages plotted as a function of $[Ca^{2+}]_i$ show that the MiRP3-induced shifts wane slightly as calcium levels are reduced (Fig. 3*F*).

*MiRP3 accelerates degradation of cellular BK.* The magnitude of MiRP3-induced shift in $V_{½\text{-act}}$ is insufficient to fully explain the reduction of BK current. This suggested MiRP3 might also regulate turnover of BK channels which was confirmed as follows: BK surface expression was quantified by labeling cell surface proteins exposed to the extracellular solution with a membrane-impermeant biotin reagent that reacts with primary amines and purification the labeled proteins via streptavidin immobilized on beads. Total and surface BK expression in transfected CHO cells were quantified without MiRP3 (vector control) and with MiRP3 (Fig. 4*A*). At steady state, MiRP3 reduced the total BK expression by 60 ± 1% and reduced surface BK protein by 75 ± 8% (means ± SD, $n = 3$).

The reduction of total and surface BK suggested MiRP3-BK complexes might have a shortened half-life. Indeed, proteolysis of the entire pool of cellular BK was accelerated by MiRP3 coexpression. The kinetics of BK expression were studied by metabolically labeling proteins with $^{35}$S-methionine and $^{35}$S-cysteine for 1 h and quantifying the expression of the total cellular and surface-expressed BK over the next 16 h. To exclude the possibility that BK expression might be attenuated nonspecifically by simple competition with MiRP3 for the protein synthetic machinery, a control was included in which BK was coexpressed with a noninteracting single-transmembrane protein, the major histocompatability antigen class II-associated invariant chain, Iip35. Figure 4*B* shows raw data from one of the three experiments used to quantify the time course for recovery of BK when coexpressed alone, with MiRP3, or with Iip35. Figure 4*C* shows the kinetics of BK for the experiment shown in 4*B*, revealing a close correlation between the decay of total channel and the surface-expressed channel in all three experimental

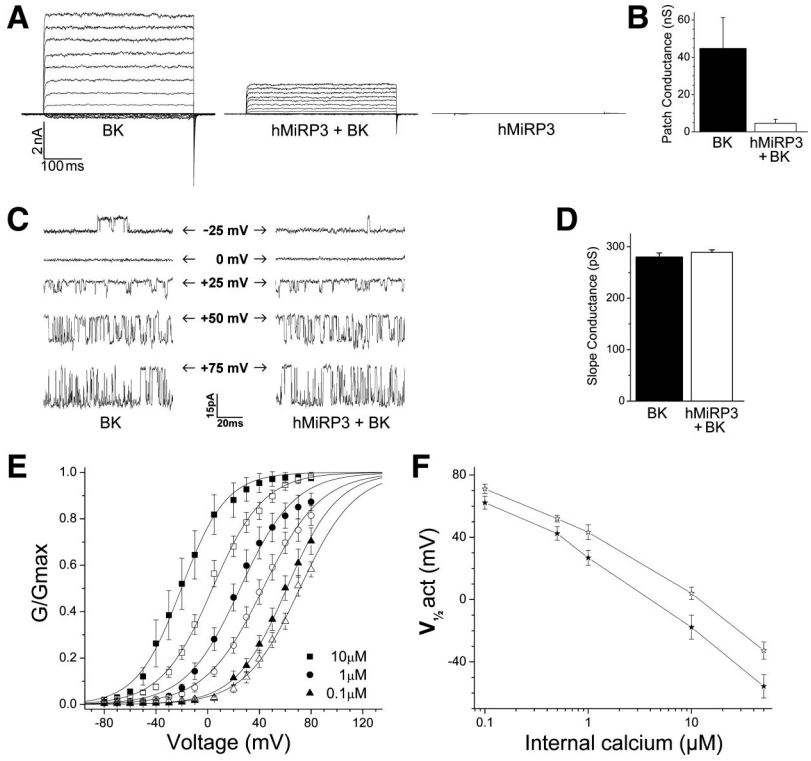


Fig. 3. Electrophysiologic effects of MiRP3 on BK currents. Patch-clamp recordings from transfected CHO cells. *A*: representative macroscopic recordings of inside-out patches from cells transfected with BK and empty vector (BK), MiRP3 and BK (hMiRP3 + BK), or MiRP3 and empty vector (hMiRP3). Voltage pulses were delivered for 400 ms at 0.4 Hz from a holding potential of −60 mV. Perfusion solution contained 10 μM free $Ca^{2+}$. *B*: mean (±SE) conductance at +80 mV is compared for patches taken from cells expressing BK or BK + MiRP3. *C*: representative single-channel recordings made from cells transfected with reduced BK cDNA. The internal membrane voltage for each recording is shown, and arrows indicate the closed state of the channels. *D*: slope conductance (±SE) is compared from single-channel recordings of BK vs. BK + MiRP3. *E*: conductance-voltage relationship for BK without or with MiRP3 at 3 different $[Ca^{2+}]_i$. Conditions were as in *A* except for varied $[Ca^{2+}]_i$ as indicated by the differently shaped symbols. Filled symbols represent values (±SE) for BK alone and open symbols for MiRP3 with BK. *F*: half-maximal activation ($V_{½\text{-act}}$) over a range of internal calcium concentrations.

groups. Coexpression with MiRP3 decreased BK half-life (total and surface) ~60% compared with BK alone or BK with Iip35 (Fig. 4*D*, $n = 3$). For all three groups, there was an ~4-h delay between the pulse and peak surface expression, as noted by Bravo-Zehnder et al. (11) in their characterization of sorting of BK to apical membrane in Madin-Darby canine kidney cells.

## DISCUSSION

The physiological roles of MiRP3 are unknown. Here, MiRP3 was localized to the apical membrane of renal IC cells and found to be coexpressed with the voltage- and calcium-activated BK channel. This prompted an evaluation that demonstrated stable interaction of MiRP3 and BK in cultured cells and two mechanisms by which MiRP3 reduces BK current: requirement for greater depolarization to open the channels (~10 mV at natural calcium concentration in IC cells), and lowered expression at the plasma membrane due to decreased BK half-life. MiRP3 is similar to other *KCNE* family proteins in altering both activation voltage and expression levels of complexes formed with classical voltage-gated potassium channels (3, 32) but is the first member found to interact with voltage- and calcium-gated BK channels.

The KCNMB accessory subunits are well-characterized modulators of BK channels that shift activation voltage either to more hyperpolarized (KCNMB1) or depolarized potentials (KCNMB4) at physiologic calcium concentrations (12, 16). As found for MiRP3, these effects wane with reduced intracellular calcium. Calcium-dependent effects of MiRP3 may be due to a direct influence on calcium binding or, as proposed for KCNMB1, the result of altered impact of calcium on activation gates and/or the effective gating charge of the voltage sensor (6, 16, 38, 44).

MiRP3 can also modify BK channel protein expression level, and this type of effect is not unprecedented for the KCNE family. MinK (encoded by *KCNE1*) can increase hERG channel expression by promoting the trafficking of channels to the cell surface (34), although enhanced degradation has not been described previously for the KCNE proteins. How might MiRP3 speed turnover of BK? Recently, BK channel surface expression was also shown to be specifically reduced by KCNMB1, as endocytosis of BK was accelerated by the accessory protein. MiRP3 might act similarly, although Toro et al. (54) saw a minimal effect on the total amount of BK channel. This difference may be due to the relatively short time scale of their immunohistochemical experiments (~1 h), which may not have allowed appreciable lysosomal degradation. Alternatively, MiRP3 may cause ubiquitinization of BK, similar to the effect of the single transmembrane-spanning protein, Vpu, which stably interacts with the potassium leak channel, K2P3 (Task-1) (22).

BK channels are widely expressed and are modulated by a variety of regulatory mechanisms depending on the cell type and physiological conditions (28). During pregnancy, the myometrium has increased mRNA and protein expression of a BK splice variant that leads to retention of channel in the endoplasmic reticulum/golgi complex, decreasing levels at the plasma membrane (64, 65). Similarly, endothelial-cell expression of caveolin-1 inhibits BK currents, perhaps by holding the channels within lipid rafts (59). As discussed above, KCNMB1 may regulate BK surface expression in some cells. Shortening the channel half-life by MiRP3 is yet another mechanism of modulating the activity of BK.

Focal expression of MiRP3 on apical membranes of IC cells underscores the fact that MinK-related peptides, like some of their pore-forming partners, can be directed to specific subcellular locations. Supporting native assembly of MiRP3 and BK

is observation of their coincident dense expression on apical membranes of selected IC cells in rabbit kidney (Fig. 1). This supposition is strengthened by a capacity for the subunits to interact stably and to alter function in cultured cells (Figs. 2–4). Direct evidence for assembly of MiRP3 and BK in mammalian kidney will require coimmunoprecipitation of the proteins from native tissue, a challenging proposition with members of the KCNE family. Finley and colleagues (17) achieved coimmunoprecipitation of MinK with KCNQ1 and ERG channels from horse heart and McCrossan et al. (33) showed that MiRP2 forms stable complexes with either Kv2.1 or Kv3.1 in rat brain. Otherwise, numerous attempts at native coprecipitation with KCNE proteins have had limited success (32). An alternative, albeit indirect, approach to validate functional association in vivo is targeted deletion of the KCNE4 gene (55, 56).

Whereas BK channels have a seventh transmembrane segment, S0 (57), they are otherwise like classical Kv voltage-gated potassium channel subunits that have six membrane spans and one pore-forming P loop and assemble as tetramers to form a central ion conduction pathway (27, 30, 45, 50). Therefore, the stoichiometry of MiRP3-BK complexes may be hexameric-like $I_{Ks}$ channels (15, 36, 58), that is, with two MiRP3 and four BK subunits.

What role might MiRP3 play in the kidney? Flow-dependent potassium secretion in the rabbit is mediated by apical BK channels in IC cells (60, 62) and subject to modifications of serum potassium concentration, such that a low potassium diet in rabbits leads to a loss of BK channels from the apical surface of IC cells and a marked reduction of flow-dependent $K^+$ secretion (37). Possible mechanisms for this effect include downregulated expression of mRNA encoding the BK alpha subunit (37), enhanced expression of KCNMB4 (18, 37), channel suppression by mitogen-activated protein kinases (26), as well as the above described effects of MiRP3. To explore this possibility, an evaluation of the effects of dietary potassium on MiRP3 expression in rabbit collecting duct is planned.

In mice, BK channels with the accessory subunit KCNMB1 are responsible for flow-dependent potassium secretion, and activity appears to be confined to the CNT upstream of the collecting duct (42, 43, 47). Because KCNMB1 is expressed only in the principal-like cells of the CNT (18), it appears as if flow-dependent kaliuresis in mice does not involve IC cells. Less is known about the modulation of this phenomenon in rats where flow-dependent kaliuresis is modulated by dietary potassium (14, 23) but there is no apparent change of BK channel activity of IC cells of the cortical collecting duct (40).

Flow-independent potassium transport involving active $H^+/K^+$ exchange in IC cells is also regulated by dietary potassium content and might involve MiRP3 modulation. Zhou and Wingo (66) demonstrated a pathway employing H-K-ATPase-dependent potassium recycling that is required when animals are fed a potassium-replete diet, presumably preventing acidosis-induced hyperkalemia. BK is likely to be the channel mediating potassium efflux in this case and channel downregulation is crucial when serum potassium levels drop. These forms of regulating $K^+$ flux in response to potassium intake raise the intriguing possibility that under potassium-deplete conditions MiRP3 could participate in the inhibition of BK activity and minimize urinary potassium loss.

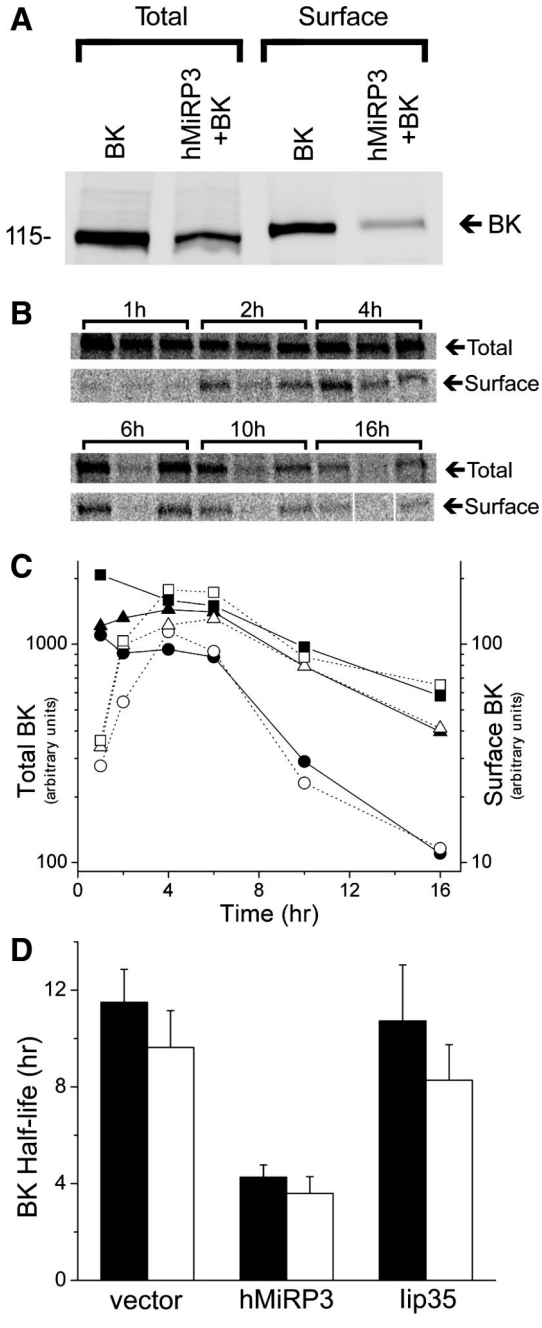


Fig. 4. MiRP3 shortens half-life of BK protein. *A*: CHO cells were transfected with wild-type BK channels and an equal concentration of either empty vector (BK) or MiRP3 (hMiRP3+BK), allowing quantification of the total and surface-expressed BK. The sample blot shows cotransfection of MiRP3 with BK leading to a 61% reduction of total BK and an 84% reduction of surface BK at steady state. *B–D*: pulse-chase experiments demonstrating enhanced degradation of cellular BK by MiRP3. *B*: phosphorimages of total cellular BK and surface-expressed BK chased for the times specified above the brackets. For each time point, the samples were loaded–from *left* to *right*–from cells expressing BK with empty vector, MiRP3, and Iip35. *C*: densities of the bands in *B* were quantified for the 16-h period (empty vector, squares; MiRP3, circles; Iip35, triangles). Arbitrary counts for total cellular expression (filled symbols) and surface expression (open symbols) are plotted to the *left* and *right* *y*-axes, respectively. *D*: half-life of BK expression for 3 experiments is plotted for total cellular expression (filled bars) and surface expression (open bars, means ± SE).

## ACKNOWLEDGMENTS

We thank S. A. Mentone for expert preparation of immunohistochemical samples, B. Zavilowitz for providing samples of rabbit kidney, E. Cepaitis for immunoprecipitation experiments, D. Cox for advice with metal chelators, and D. Goldstein and T. Yorke for careful review of the manuscript.

## GRANTS

This work was funded by grants from the National Institutes of Health to S. A. N. Goldstein and D. I. Levy, and the National Kidney Foundation to D. I. Levy.

## REFERENCES

1. **Abbott GW, Butler MH, Bendahhou S, Dalakas MC, Ptacek LJ, Goldstein SA.** MiRP2 forms potassium channels in skeletal muscle with Kv3.4 and is associated with periodic paralysis. *Cell* 104: 217–231, 2001.
2. **Abbott GW, Goldstein SA.** Disease-associated mutations in *KCNE* potassium channel subunits (MiRPs) reveal promiscuous disruption of multiple currents and conservation of mechanism. *FASEB J* 16: 390–400, 2002.
3. **Abbott GW, Goldstein SA.** A superfamily of small potassium channel subunits: form and function of the MinK-related peptides (MiRPs). *Q Rev Biophys* 31: 357–398, 1998.
4. **Abbott GW, Sesti F, Splawski I, Buck ME, Lehmann MH, Timothy KW, Keating MT, Goldstein SA.** MiRP1 forms $I_{Kr}$ potassium channels with HERG and is associated with cardiac arrhythmia. *Cell* 97: 175–187, 1999.
5. **Alper SL, Stuart-Tilley AK, Biemesderfer D, Shmukler BE, Brown D.** Immunolocalization of AE2 anion exchanger in rat kidney. *Am J Physiol Renal Physiol* 273: F601–F614, 1997.
6. **Bao L, Cox DH.** Gating and ionic currents reveal how the $BK_{Ca}$ channel's $Ca^{2+}$ sensitivity is enhanced by its β1 subunit. *J Gen Physiol* 126: 393–412, 2005.
7. **Bendahhou S, Marionneau C, Haurogne K, Larroque MM, Derand R, Szuts V, Escande D, Demolombe S, Barhanin J.** In vitro molecular interactions and distribution of KCNE family with KCNQ1 in the human heart. *Cardiovasc Res* 67: 529–538, 2005.
8. **Biemesderfer D, Dekan G, Aronson PS, Farquhar MG.** Assembly of distinctive coated pit and microvillar microdomains in the renal brush border. *Am J Physiol Renal Fluid Electrolyte Physiol* 262: F55–F67, 1992.
9. **Biemesderfer D, Rutherford PA, Nagy T, Pizzonia JH, Abu-Alfa AK, Aronson PS.** Monoclonal antibodies for high-resolution localization of NHE3 in adult and neonatal rat kidney. *Am J Physiol Renal Physiol* 273: F289–F299, 1997.
10. **Bockenhauer D, Zilberberg N, Goldstein SA.** KCNK2: reversible conversion of a hippocampal potassium leak into a voltage-dependent channel. *Nat Neurosci* 4: 486–491, 2001.
11. **Bravo-Zehnder M, Orio P, Norambuena A, Wallner M, Meera P, Toro L, Latorre R, Gonzalez A.** Apical sorting of a voltage- and $Ca^{2+}$-activated $K^+$ channel alpha-subunit in Madin-Darby canine kidney cells is independent of N-glycosylation. *Proc Natl Acad Sci USA* 97: 13114–13119, 2000.
12. **Brenner R, Jegla TJ, Wickenden A, Liu Y, Aldrich RW.** Cloning and functional characterization of novel large conductance calcium-activated potassium channel β subunits, hKCNMB3 and hKCNMB4. *J Biol Chem* 275: 6453–6461, 2000.
13. **Busch AE, Varnum MD, North RA, Adelman JP.** An amino acid mutation in a potassium channel that prevents inhibition by protein kinase C. *Science* 255: 1705–1707, 1992.
14. **Cheema-Dhadli S, Lin SH, Chong CK, Kamel KS, Halperin ML.** Requirements for a high rate of potassium excretion in rats consuming a low electrolyte diet. *J Physiol* 572: 493–501, 2006.
15. **Chen H, Kim LA, Rajan S, Xu S, Goldstein SA.** Charybdotoxin binding in the $I_{Ks}$ pore demonstrates two MinK subunits in each channel complex. *Neuron* 40: 15–23, 2003.
16. **Cox DH, Aldrich RW.** Role of the beta1 subunit in large-conductance $Ca^{2+}$-activated $K^+$ channel gating energetics. Mechanisms of enhanced $Ca^{2+}$ sensitivity. *J Gen Physiol* 116: 411–432, 2000.
17. **Finley MR, Li Y, Hua F, Lillich J, Mitchell KE, Ganta S, Gilmour RF Jr, Freeman LC.** Expression and coassociation of ERG1, KCNQ1, and KCNE1 potassium channel proteins in horse heart. *Am J Physiol Heart Circ Physiol* 283: H126–H138, 2002.
18. **Grimm PR, Foutz RM, Brenner R, Sansom SC.** Identification and localization of BK-beta subunits in the distal nephron of the mouse kidney. *Am J Physiol Renal Physiol* 293: F350–F359, 2007.
19. **Grunnet M, Jespersen T, Rasmussen HB, Ljungstrom T, Jorgensen NK, Olesen SP, Klaerke DA.** KCNE4 is an inhibitory subunit to the KCNQ1 channel. *J Physiol* 542: 119–130, 2002.
20. **Grunnet M, Rasmussen HB, Hay-Schmidt A, Rosenstierne M, Klaerke DA, Olesen SP, Jespersen T.** KCNE4 is an inhibitory subunit to Kv1.1 and Kv1.3 potassium channels. *Biophys J* 85: 1525–1537, 2003.
21. **Harlow E, Lane D.** *Antibodies: A Laboratory Manual*. Cold Spring Harbor, NY: Cold Spring Harbor Laboratory, 1988.
22. **Hsu K, Seharaseyon J, Dong P, Bour S, Marban E.** Mutual functional destruction of HIV-1 Vpu and host TASK-1 channel. *Mol Cell* 14: 259–267, 2004.
23. **Khuri RN, Strieder WN, Giebisch G.** Effects of flow rate and potassium intake on distal tubular potassium transfer. *Am J Physiol* 228: 1249–1261, 1975.
24. **Kim J, Kim YH, Cha JH, Tisher CC, Madsen KM.** Intercalated cell subtypes in connecting tubule and cortical collecting duct of rat and mouse. *J Am Soc Nephrol* 10: 1–12, 1999.
25. **Kim LA, Furst J, Butler MH, Xu S, Grigorieff N, Goldstein SA.** $I_{to}$ channels are octomeric complexes with four subunits of each Kv4.2 and $K^+$ channel-interacting protein 2. *J Biol Chem* 279: 5549–5554, 2004.
26. **Li D, Wang Z, Sun P, Jin Y, Lin DH, Hebert SC, Giebisch G, Wang WH.** Inhibition of MAPK stimulates the $Ca^{2+}$-dependent big-conductance K channels in cortical collecting duct. *Proc Natl Acad Sci USA* 103: 19569–19574, 2006.
27. **Long SB, Campbell EB, Mackinnon R.** Crystal structure of a mammalian voltage-dependent Shaker family $K^+$ channel. *Science* 309: 897–903, 2005.
28. **Lu R, Alioua A, Kumar Y, Eghbali M, Stefani E, Toro L.** MaxiK channel partners: physiological impact. *J Physiol* 570: 65–72, 2006.
29. **Lundquist AL, Manderfield LJ, Vanoye CG, Rogers CS, Donahue BS, Chang PA, Drinkwater DC, Murray KT, George AL Jr.** Expression of multiple KCNE genes in human heart may enable variable modulation of $I_{Ks}$. *J Mol Cell Cardiol* 38: 277–287, 2005.
30. **MacKinnon R.** Determination of the subunit stoichiometry of a voltage-activated potassium channel. *Nature* 350: 232–235, 1991.
31. **Manderfield LJ, George AL Jr.** KCNE4 can co-associate with the $I_{Ks}$ (KCNQ1-KCNE1) channel complex. *FEBS J* 275: 1336–1349, 2008.
32. **McCrossan ZA, Abbott GW.** The MinK-related peptides. *Neuropharmacology* 47: 787–821, 2004.
33. **McCrossan ZA, Lewis A, Panaghie G, Jordan PN, Christini DJ, Lerner DJ, Abbott GW.** MinK-related peptide 2 modulates Kv2.1 and Kv3.1 potassium channels in mammalian brain. *J Neurosci* 23: 8077–8091, 2003.
34. **McDonald TV, Yu Z, Ming Z, Palma E, Meyers MB, Wang KW, Goldstein SA, Fishman GI.** A minK-HERG complex regulates the cardiac potassium current $I_{Kr}$. *Nature* 388: 289–292, 1997.
35. **Misonou H, Menegola M, Buchwalder L, Park EW, Meredith A, Rhodes KJ, Aldrich RW, Trimmer JS.** Immunolocalization of the $Ca^{2+}$-activated $K^+$ channel Slo1 in axons and nerve terminals of mammalian brain and cultured neurons. *J Comp Neurol* 496: 289–302, 2006.
36. **Morin TJ, Kobertz WR.** Counting membrane-embedded KCNE β-subunits in functioning $K^+$ channel complexes. *Proc Natl Acad Sci USA* 105: 1478–1482, 2008.
37. **Najjar F, Zhou H, Morimoto T, Bruns JB, Li HS, Liu W, Kleyman TR, Satlin LM.** Dietary $K^+$ regulates apical membrane expression of maxi-K channels in rabbit cortical collecting duct. *Am J Physiol Renal Physiol* 289: F922–F932, 2005.
38. **Orio P, Latorre R.** Differential effects of β1 and β2 subunits on BK channel activity. *J Gen Physiol* 125: 395–411, 2005.
39. **Pacha J, Frindt G, Sackin H, Palmer LG.** Apical maxi K channels in intercalated cells of CCT. *Am J Physiol Renal Fluid Electrolyte Physiol* 261: F696–F705, 1991.
40. **Palmer LG, Frindt G.** High-conductance K channels in intercalated cells of the rat distal nephron. *Am J Physiol Renal Physiol* 292: F966–F973, 2007.
41. **Patton C, Thompson S, Epel D.** Some precautions in using chelators to buffer metals in biological solutions. *Cell Calcium* 35: 427–431, 2004.
42. **Pluznick JL, Sansom SC.** BK channels in the kidney: role in $K^+$ secretion and localization of molecular components. *Am J Physiol Renal Physiol* 291: F517–F529, 2006.

43. **Pluznick JL, Wei P, Grimm PR, Sansom SC.** BK-β1 subunit: immunolocalization in the mammalian connecting tubule and its role in the kaliuretic response to volume expansion. *Am J Physiol Renal Physiol* 288: F846–F854, 2005.
44. **Qian X, Magleby KL.** Beta1 subunits facilitate gating of BK channels by acting through the $Ca^{2+}$, but not the $Mg^{2+}$, activating mechanisms. *Proc Natl Acad Sci USA* 100: 10061–10066, 2003.
45. **Quirk JC, Reinhart PH.** Identification of a novel tetramerization domain in large conductance $K_{Ca}$ channels. *Neuron* 32: 13–23, 2001.
46. **Radicke S, Cotella D, Graf EM, Banse U, Jost N, Varro A, Tseng GN, Ravens U, Wettwer E.** Functional modulation of the transient outward current Ito by KCNE beta-subunits and regional distribution in human nonfailing and failing hearts. *Cardiovasc Res* 71: 695–703, 2006.
47. **Rieg T, Vallon V, Sausbier M, Sausbier U, Kaissling B, Ruth P, Osswald H.** The role of the BK channel in potassium homeostasis and flow-induced renal potassium excretion. *Kidney Int* 72: 566–573, 2007.
48. **Schulze-Bahr E, Wang Q, Wedekind H, Haverkamp W, Chen Q, Sun Y, Rubie C, Hordt M, Towbin JA, Borggrefe M, Assmann G, Qu X, Somberg JC, Breithardt G, Oberti C, Funke H.** *KCNE1* mutations cause Jervell and Lange-Nielsen syndrome. *Nat Genet* 17: 267–268, 1997.
49. **Sesti F, Abbott GW, Wei J, Murray KT, Saksena S, Schwartz PJ, Priori SG, Roden DM, George AL Jr, Goldstein SA.** A common polymorphism associated with antibiotic-induced cardiac arrhythmia. *Proc Natl Acad Sci USA* 97: 10613–10618, 2000.
50. **Shen KZ, Lagrutta A, Davies NW, Standen NB, Adelman JP, North RA.** Tetraethylammonium block of Slowpoke calcium-activated potassium channels expressed in *Xenopus* oocytes: evidence for tetrameric channel formation. *Pflügers Arch* 426: 440–445, 1994.
51. **Splawski I, Tristani-Firouzi M, Lehmann MH, Sanguinetti MC, Keating MT.** Mutations in the h*minK* gene cause long QT syndrome and suppress $I_{Ks}$ function. *Nat Genet* 17: 338–340, 1997.
52. **Teng-umnuay P, Verlander JW, Yuan W, Tisher CC, Madsen KM.** Identification of distinct subpopulations of intercalated cells in the mouse collecting duct. *J Am Soc Nephrol* 7: 260–274, 1996.
53. **Teng S, Ma L, Zhen Y, Lin C, Bahring R, Vardanyan V, Pongs O, Hui R.** Novel gene h*KCNE4* slows the activation of the KCNQ1 channel. *Biochem Biophys Res Commun* 303: 808–813, 2003.
54. **Toro B, Cox N, Wilson RJ, Garrido-Sanabria E, Stefani E, Toro L, Zarei MM.** KCNMB1 regulates surface expression of a voltage and $Ca^{2+}$-activated $K^+$ channel via endocytic trafficking signals. *Neuroscience* 142: 661–669, 2006.
55. **Vallon V, Grahammer F, Richter K, Bleich M, Lang F, Barhanin J, Volkl H, Warth R.** Role of KCNE1-dependent $K^+$ fluxes in mouse proximal tubule. *J Am Soc Nephrol* 12: 2003–2011, 2001.
56. **Vetter DE, Mann JR, Wangemann P, Liu J, McLaughlin KJ, Lesage F, Marcus DC, Lazdunski M, Heinemann SF, Barhanin J.** Inner ear defects induced by null mutation of the *Isk* gene. *Neuron* 17: 1251–1264, 1996.
57. **Wallner M, Meera P, Toro L.** Determinant for beta-subunit regulation in high-conductance voltage-activated and $Ca^{2+}$-sensitive $K^+$ channels: an additional transmembrane region at the N terminus. *Proc Natl Acad Sci USA* 93: 14922–14927, 1996.
58. **Wang KW, Goldstein SA.** Subunit composition of minK potassium channels. *Neuron* 14: 1303–1309, 1995.
59. **Wang XL, Ye D, Peterson TE, Cao S, Shah VH, Katusic ZS, Sieck GC, Lee HC.** Caveolae targeting and regulation of large conductance $Ca^{2+}$-activated $K^+$ channels in vascular endothelial cells. *J Biol Chem* 280: 11656–11664, 2005.
60. **Woda CB, Bragin A, Kleyman TR, Satlin LM.** Flow-dependent $K^+$ secretion in the cortical collecting duct is mediated by a maxi-K channel. *Am J Physiol Renal Physiol* 280: F786–F793, 2001.
61. **Woda CB, Leite M Jr, Rohatgi R, Satlin LM.** Effects of luminal flow and nucleotides on $[Ca^{2+}]_i$ in rabbit cortical collecting duct. *Am J Physiol Renal Physiol* 283: F437–F446, 2002.
62. **Woda CB, Miyawaki N, Ramalakshmi S, Ramkumar M, Rojas R, Zavilowitz B, Kleyman TR, Satlin LM.** Ontogeny of flow-stimulated potassium secretion in rabbit cortical collecting duct: functional and molecular aspects. *Am J Physiol Renal Physiol* 285: F629–F639, 2003.
63. **Xu DL, Martin PY, Ohara M, St John J, Pattison T, Meng X, Morris K, Kim JK, Schrier RW.** Upregulation of aquaporin-2 water channel expression in chronic heart failure rat. *J Clin Invest* 99: 1500–1505, 1997.
64. **Zarei MM, Eghbali M, Alioua A, Song M, Knaus HG, Stefani E, Toro L.** An endoplasmic reticulum trafficking signal prevents surface expression of a voltage- and $Ca^{2+}$-activated $K^+$ channel splice variant. *Proc Natl Acad Sci USA* 101: 10072–10077, 2004.
65. **Zarei MM, Zhu N, Alioua A, Eghbali M, Stefani E, Toro L.** A novel MaxiK splice variant exhibits dominant-negative properties for surface expression. *J Biol Chem* 276: 16232–16239, 2001.
66. **Zhou X, Wingo CS.** Stimulation of total $CO_2$ flux by 10% $CO_2$ in rabbit CCD: role of an apical Sch-28080- and Ba-sensitive mechanism. *Am J Physiol Renal Fluid Electrolyte Physiol* 267: F114–F120, 1994.